Influence of nonlinear turbulent friction on the system frequency response in transient pipe flow modelling and analysis

HUAN-FENG DUAN (IAHR Member), Assistant Professor, *Department of Civil and Environmental Engineering, Hong Kong Polytechnic University, Hung Hom, Kowloon, Hong Kong*

Email: hf.duan@polyu.edu.hk (author for correspondence)

TONG-CHUAN CHE, PhD Student, *Department of Civil and Environmental Engineering, Hong Kong Polytechnic University, Hung Hom, Kowloon, Hong Kong*

Email: tong-chuan.che@connect.polyu.hk

PEDRO J. LEE (IAHR Member), Associate Professor, *Department of Civil and Natural Resources Engineering, University of Canterbury, New Zealand*

Email: pedro.lee@canterbury.ac.nz

MOHAMED S. GHIDAOUI (IAHR Member), Chair Professor, *Department of Civil and Environmental Engineering, Hong Kong University of Science and Technology, Clear Water Bay, Kowloon, Hong Kong*

Email: ghidaoui@ust.hk

Running Head: Nonlinear transient frequency response modelling and analysis

Influence of nonlinear turbulent friction on the system frequency response in transient pipe flow modelling and analysis

ABSTRACT

The system frequency response (SFR) based method has been widely developed and applied for the modelling of transient pipe flow and the assessment of pipeline system conditions. The linearization assumption is commonly imposed for the nonlinear turbulent friction term in the SFR model. Previous studies have demonstrated the impact of the linearization approximation on the accuracy of the SFR-based modelling and analysis. This paper aims to improve the traditional SFR-based method by incorporating the nonlinear component of the friction term in a two-step analytical extension of the SFR expression. Numerical comparisons with the Method of Characteristic (MOC) highlight the improved accuracy that the extended SFR result provides over the traditional approach under various flow conditions.

Keywords: Nonlinear turbulent friction; relative importance; system frequency response; transfer matrix; transient

1 Introduction

Transient waves are fast moving elastic shocks that travel at high speeds in pipeline systems (e.g., around 1000 m/s in elastic pipelines). They are generally triggered by planned or accidental flow changing events in pipe fluid systems. Transient events may be caused by fast operations of valves, starting and stopping of pumps and variations in the supply or demand of the system fluid. These sudden changes in system flow require the imposition of large forces to accelerate or decelerate the fluid, and consequently are capable of inducing severe or even catastrophic pressures in the pipeline. In engineering practice across a multitude of fluids systems and applications, transient flows exert decisive influences on practical aspects of engineering design and operation of pipeline systems, such as structural (e.g., pipe broken) and functional (e.g., pollutant intrusion) integrities of pipelines (Chaudhry, 1987; Duan, Tung, & Ghidaoui, 2010; Ghidaoui, Zhao, McInnis, & Axworthy, 2005; Meniconi et al., 2015; Meniconi, Brunone, Ferrante, & Massari, 2011; Wylie, Streeter, & Suo, 1993).

It was found that small magnitude transient waves can be used as a source of information in pipeline integrity management applications as they can move rapidly throughout a pipeline system and their waveforms are modified by their propagation and reflection interactions with the pipe network components, (Colombo, Lee, & Karney, 2009). Recently developed techniques for leakage and blockage detection in water pipeline systems are utilizing the information associated with the transient damping and reflections (Brunone, 1999; Covas, Ramos, Graham, & Maksimovic, 2005; Duan, Lee, Ghidaoui, & Tuck, 2014;

Duan, Lee, Ghidaoui, & Tung, 2010, 2011, 2012a; Duan et al., 2013; Ferrante & Brunone, 2003; Gong, Lambert, Zecchin, & Simpson, 2016; Lee, Duan, Ghidaoui, & Karney, 2013; Lee, Lambert, Simpson, Vítkovský, & Liggett, 2006; Sattar & Chaudhry, 2008; Vítkovský, Simpson, & Lambert, 2000; Wang, Lambert, Simpson, Liggett, & Vítkovský, 2002). Utilization of transient data for leak detection could have great practical significance since pipe leakage is a common and costly water conservation and health issue in urban water supply systems worldwide. Consequently, a reliable modelling and analysis of transient flows in pipes is important to advancing the practical utilization of transients as a source of information and, at the same time, minimizing their damaging impacts on the physical infrastructures.

The modelling and analysis of transient pipe flows are usually performed in the time domain by various numerical schemes that are widely developed in the literature, for example, the commonly used Method of Characteristics (MOC) (Chaudhry, 1987). In this model, the pipeline system needs to be discretized by following relevant requirements of numerical stability and convergence so that the average state and time evolution of transient waves along the pipeline are calculated accurately. Unfortunately, the efficiency of the time domain simulation is greatly affected by the applied numerical scheme and the system complexity, especially when a physically-based unsteady friction model is included in the modelling (Duan, Ghidaoui, Lee, & Tung, 2010; Ghidaoui & Mansour, 2002; Vardy & Brown, 1995; Vítkovský, Stephens, Bergant, Simpson, & Lambert, 2006; Wylie et al., 1993). Another commonly used method for the simulation and analysis of transient pipe flows is the frequency domain analysis. Various types of frequency domain analysis have been developed in the literature, including system frequency response (SFR) method, impedance matrix (IM) method and impulse response (IR) method (Kim, 2007; Lee, Duan, Ghidaoui, et al., 2013; Vítkovský, Lee, Zecchin, Simpson, & Lambert, 2011; Zecchin, Lambert, Simpson, & White, 2010). The accuracy of frequency domain analyses is affected by the linearization approximation of complex effects such as turbulent friction and valve dynamics. Lee and Vítkovský (2010) quantified systematically the linearization errors of the valve operation and steady friction effect in the frequency domain analysis for transient modelling. Lee, Duan, Vítkovský, Zecchin, and Ghidaoui (2013) investigated the inaccuracy of the transient line modelling due to the discretization in both time and frequency domains. Furthermore, the study of Lee (2013) also indicated that the transmission line model deviates significantly from the MOC when the system dynamics are represented in a head-flow plot, with the difference increasing with the wave magnitude. These previous results have demonstrated the significance of the linearization approximation in the current frequency domain analysis methods.

In recent years, the frequency domain analysis method has become more popular for the diagnosis and analysis of transient pipe flow systems and also in pipeline condition assessment (leakage and blockage detection) (Duan & Lee, 2016; Duan et al., 2014; Duan et al., 2011; Duan, Lee, et al., 2012a; Duan, Lee, Ghidaoui, & Tung, 2012b; Duan et al., 2013; Ghazali, Beck, Shucksmith, Boxall, & Staszewski, 2012; Gong et al., 2016; Lee, Vítkovský, Lambert, Simpson, & Liggett, 2005). Particularly, transient responses of various pipe defects (leakage and/or blockage) could be efficiently incorporated into the frequency domain model, and their impact on the response can be separated from other system effects. These defects can be identified and detected inversely through this process. For example, the SFR-based method has been developed and used in the literature for the detection of pipe leakage and blockage as well as unknown branches in pipe systems (Duan & Lee, 2016; Lee, Duan, Ghidaoui, et al., 2013). Again, these applications have demonstrated that the accuracy of frequency domain analysis for pipe system diagnosis is of great importance and the linearization approximations imposed in the development of these methods will need to be studied in greater depth. The aim of this paper is to develop a method for mitigating the errors associated with the linear approximation in the frequency domain models such that nonlinear friction effect and complex device operations can be accurately represented and modelled.

This paper first derives and extends the SFR method by including the nonlinear turbulent friction effect and the results are compared to the original linearized SFR method and the MOC-based numerical results. Finally, the results and findings of this study are discussed in terms of the accuracy in transient pipe flow modelling as well as the practical implications of transient system analysis (such as pipeline diagnosis) in urban water pipeline systems.

2 Models and methods

For clarity, the transient flow models, analysis methods, as well as the common assumptions used in previous studies are summarized and presented in this section.

2.1 One-dimensional transient model

The one-dimensional (1D) transient model is used in this study for the time domain numerical simulation and frequency domain analytical analysis, with the governing equations given by (Chaudhry, 1987; Wylie et al., 1993):

$$\frac{gA}{a^2}\frac{\partial H}{\partial t}+\frac{\partial Q}{\partial x}=0 \tag{1}$$

$$\frac{\partial Q}{\partial t}+gA\frac{\partial H}{\partial x}+\frac{\pi D}{\rho}\tau_w=0 \tag{2}$$

where H is pressure head; Q is flowrate; a is wavespeed; t is time; x is spatial coordinate along pipeline; D is pipe diameter; A is pipe cross-sectional area; g is gravitational acceleration; ρ is fluid (water) density; τ_w is pipe wall shear stress, which can be divided into two parts as (Vardy & Brown, 1995; Zielke, 1968):

$$\tau_w = \tau_{ws} + \tau_{wu} \tag{3}$$

with τ_{ws} and τ_{wu} being the quasi-steady and unsteady components of τ_w, respectively. For turbulent flows, the quasi-steady wall shear stress is commonly simulated by the Darcy-Weisbach equation as (Ghidaoui et al., 2005),

$$\tau_{ws} = \frac{\rho f}{8A^2} Q|Q| = sign(Q)\frac{\rho f Q^2}{8A^2} \tag{4}$$

with f being the Darcy friction factor at initial flow state and $sign()$ for the sign function. For modelling the unsteady wall shear stress, the weighting function based (WFB) model is adopted in this study, which is given by (Vardy & Brown, 1995, 2003),

$$\tau_{wu} = \frac{4\rho\nu}{DA}\int_0^t W(t-t')\frac{\partial Q(t')}{\partial t'}dt' \tag{5}$$

where $W(t) = \phi e^{-\lambda t}/\sqrt{\pi t}$ is weighting function with ϕ, λ being convolution coefficients for various flow regimes, with $\phi = D/4\sqrt{\nu}$, $\lambda = (0.54\nu k_R)/D^2$ and $k_R = \mathrm{Re}^{\log(14.3/\mathrm{Re}^{0.05})}$; $\mathrm{Re} = QD/Av$ is Reynolds number; v is kinematic viscosity; and t' is a dummy time variable.

The MOC scheme is used for the 1D numerical simulation in the time domain (Chaudhry, 1987), where the nonlinear turbulent friction term in Eq. (4) is treated discretely by a 2nd-order approximation and the unsteady friction term in Eq. (5) is dealt with by the full convolution of historical time effect (Vardy & Brown, 1995; Wylie et al., 1993). The MOC-based numerical simulation method has been widely studied and fully validated for its accuracy and validity in the literature (Ghidaoui et al., 2005) and is used as the benchmark for the evaluation of the extended SFR-based results in this study.

2.2 SFR result by transfer matrix method

The frequency domain equivalence of the 1D transient model can be obtained by applying the transfer matrix analysis after considering the linearization of the turbulent friction term, and the results can be obtained as follows (Chaudhry, 1987; Lee et al., 2006):

$$\begin{Bmatrix} q^* \\ h^* \end{Bmatrix}^D = \begin{bmatrix} \cosh(i\mu l) & \frac{1}{Z}\sinh(i\mu l) \\ Z\sinh(i\mu l) & \cosh(i\mu l) \end{bmatrix} \begin{Bmatrix} q^* \\ h^* \end{Bmatrix}^U \tag{6}$$

where q^*, h^* are transient flowrate and head in the frequency domain; l is the length of uniform pipe section; superscripts 'U, D' indicate the quantities for upstream and downstream ends of uniform pipe section; i is the imaginary unit; μ is wave propagation operator; Z is characteristic impedance. Considering the linearized steady friction effect,

$$\mu = \frac{\omega}{a}\sqrt{1-iR_s}\ ;\ Z = -\frac{a}{gA}\sqrt{1-iR_s} \tag{7}$$

where ω is frequency; R_s is linearized steady friction resistance factor, and (Lee et al., 2006; Mpesha, Gassman, & Chaudhry, 2001; Sattar & Chaudhry, 2008; Wang et al., 2002),

$$R_s = \frac{fQ_0}{\omega DA} \tag{8}$$

Note that the steady friction term for turbulence pipe flows is 2nd-order nonlinear, which is very difficult to be converted directly into the frequency domain, and therefore a linearization of this term has been applied for obtaining the above results. That is, it assumes that $q_t << Q_0$, or $q_t^* = q_t/(Q_0 + q_t) << 1$, where q_t and Q_0 are the transient flow part and the initially steady (pre-transient) flow part, and q_t^* is the percentage of transient part in the total flow, so that in Eq. (4),

$$Q^2 = \left(Q_0 + q_t\right)^2 \approx Q_0^2 + 2Q_0 q_t \tag{9}$$

As a result, the nonlinear turbulent friction term in Eq. (4) is simplified into a linear function for the cases of small-amplitude transient flows, which can then be explicitly converted into the frequency domain by Fourier transform, as given in Eq. (8) (Lee et al., 2006).

Particularly, for the simple pipe system in Fig. 1, the SFR can be obtained by applying the boundary conditions to Eq. (6) and the transient pressure head is given as (Duan et al., 2011; Lee, Duan, Ghidaoui, et al., 2013; Lee et al., 2006),

$$h^* = Z\frac{\sinh\left(i\mu l\right)}{\cosh\left(i\mu l\right)} \tag{10}$$

Note that Eq. (10) represents the transient response (pressure head) per unit input perturbation (e.g., unit discharge variation at the downstream end in Fig. 1). The nonlinearity of the valve orifice relationship is not considered in the following study, in order to highlight and investigate the nonlinear friction effect in this paper. To this end, a known discharge curve (as shown in Fig. 1) is imposed to the downstream end.

3 Extended SFR for Nonlinear Turbulent Friction

Considering the nonlinear turbulent friction term as in Eq. (4), and applying the similar frequency domain analysis procedure (note: the detailed derivation process is provided in the appendix), the transfer matrix result can be extended and obtained (termed as extended SFR result, denoted by subscript "*E*" in this paper) as follows (i.e., Eq. (A.30) in the appendix):

$$\begin{Bmatrix} q^* \\ h^* \end{Bmatrix}^D = \begin{bmatrix} \cosh(i\mu_E l) & \frac{1}{Z_E}\sinh(i\mu_E l) \\ Z_E \sinh(i\mu_E l) & \cosh(i\mu_E l) \end{bmatrix} \begin{Bmatrix} q^* \\ h^* \end{Bmatrix}^U \tag{11}$$

where μ_E and Z_E are transient wave propagation operator/coefficient and characteristic impedance for the extended SFR result, and

$$\mu_E = \frac{\omega}{a}\sqrt{1-iR_E}\ ,\ Z_E = -\frac{a}{gA}\sqrt{1-iR_E} \tag{12}$$

in which R_E is the extended friction resistance factor, and

$$R_E = R_{s1} + R_{s2} + R_u \tag{13}$$

with R_{s1} and R_{s2} being the linear (1st-order) and nonlinear (2nd-order) steady components of extended friction resistance factor; R_u being the unsteady friction resistance factor. The derivations of these factors are provided in the appendix. Specifically, from Eq. (A.22) given in the appendix, it has,

$$R_{s1} = \frac{fQ_0}{\omega DA}\ ;\ R_{s2} = \frac{fq_0}{2\omega DA}\ ;\ R_u = \frac{16i\nu\phi}{D^2\sqrt{\lambda + i\omega}} \tag{14}$$

where q_0 is the initial flow change for generating transient (i.e., induced transient flow part). The relative importance of these different frictional components to the transient modelling is analyzed in details later in this study. Accordingly, the extended SFR result of the transient pressure head can be obtained for the simple pipe system in Fig. 1 as,

$$h_E^* = Z_E \frac{\sinh(i\mu_E l)}{\cosh(i\mu_E l)} \tag{15}$$

This result clearly shows the only difference between the original and extended SFR results is the influence of nonlinear turbulent friction to the transient characteristic impedance (Z_E) and wave propagation coefficient (μ_E). This influence is analyzed in details later in this paper.

4 Scaling Analysis of Different Friction Component Effects

Based on the derived results of the extended SFR in Eq. (11) through Eq. (14), the scaling analysis can be conducted as in the previous study of Duan, Ghidaoui, Lee, and Tung (2012). The scaling analysis results of Eq. (14) are summarized as follows:

(1) For quasi-steady friction effect:

$$R_{s1} \sim f\mathrm{Re}_0 \frac{T_w}{T_d} = f\mathrm{M}\frac{L}{D};\ R_{s2} \sim f\mathrm{Re}_{t0}\frac{T_w}{T_d} \tag{16}$$

where $\mathrm{Re}_0 = Q_0 D/Av$ is Reynolds number for initially steady (pre-transient) state; $\mathrm{Re}_{t0} = |q_0|D/Av$ is the critical Reynolds number for the generated transient flow state; $\mathrm{M} = Q_0/Aa$ is Mach number; $T_w \sim 1/\omega \sim L/a$ is longitudinal wave time scale; and $T_d \sim D^2/v$ is radial kinematic (turbulent) diffusion time scale. Note that Re_{t0} represents the corresponding transient extent occurred in the system.

(2) For unsteady friction effect, its importance is dependent on the flow condition parameter λ, which is function of T_d and Re_0, in the WFB model of Eq. (5), as:

(2.1) if ($\mathrm{Re}_0 T_w/T_d \sim Q_0 L/aAD$) <<1, then,

$$R_u \sim \sqrt{\frac{T_w}{T_d}} \tag{17a}$$

and therefore, $R_u > R_s = R_{s1} + R_{s2}$ according to Eq. (16), which means the unsteady friction component becomes more important to the wave envelope attenuation than the total quasi-steady friction effects (including linear and nonlinear parts);

(2.2) otherwise for ($\mathrm{Re}_0 T_w/T_d \sim Q_0 L/aAD$) ~ 1 or >> 1,

$$R_u \sim \frac{1}{\mathrm{Re}_0}\frac{T_d}{T_w} \tag{17b}$$

which results in $R_u < R_s = R_{s1} + R_{s2}$. Under this condition, the quasi-steady friction effect is more significant than the unsteady component in the transient modelling.

In fact, this analysis result in Eq. (16) and Eq. (17) is consistent with the well-known behaviours of transient pipe flows that the nonlinear friction effect (R_{s2}) relies largely on the generated transient intensity (Re_{t0}) and the system scale conditions (T_w/T_d), but has little relationship with the initial (pre-transient) flow condition (Wang et al., 2002; Zecchin et al., 2010). However, this result is different from the previous findings in the literature with regard to the effect of linear steady and unsteady components that depend potentially on both the pre-transient and transient conditions (Chaudhry, 1987; Duan, Ghidaoui, et al., 2012; Vardy

& Brown, 1995). Based on the analysis of transient mechanism and evolution process in Duan, Ghidaoui, et al. (2012), this obtained result demonstrates that the nonlinear component of steady friction affects mainly the instantaneous change of the transient trace envelops (e.g., pressure head) by suppressing effect of the generated transient turbulence and radial diffusion on the transient change (for example, pressure head recovering during the decelerating flow stage) during the successive wave-front passes. Therefore, the inclusion of this nonlinear friction term is important to further the understanding of the complex physics of transient pipe flows, especially for transient wave-turbulence interaction.

Furthermore, based on the derived analytical results, the relative contribution (denoted herein by η) of the nonlinear (2^{nd}-order) term to the total quasi-steady friction damping (1^{st}-order and 2^{nd}-order) can be evaluated simply by the ratio of these respective resistance factors, as

$$\eta = \frac{R_{s2}}{R_{s1} + R_{s2}} = \frac{q_0}{2Q_0 + q_0} = \frac{\mathrm{Re}_{t0}}{2\mathrm{Re}_0 + \mathrm{Re}_{t0}} \tag{18}$$

Clearly, the result of Eq. (18) implies the relative importance and contribution of the nonlinear steady friction term to the total frictional damping is highly dependent on the ratio of the generated transient intensity to the initial (pre-transient) pipe discharge. Moreover, the result of Eq. (18) also gives an implication on the assumption used in the linearized SFR result of Eq. (7), that is, η <<1 (or q_0 << Q_0) for giving Eq. (9), so that the nonlinear steady friction effect can be ignored as conducted in many previous studies (Duan et al., 2011; Ferrante & Brunone, 2003; Lee et al., 2006; Mpesha et al., 2001; Sattar & Chaudhry, 2008). On this point, the accuracy and validity of the linearization approximation applied originally for the linear SFR method is basically governed by the parameter η herein.

Consequently, the above analytical results and analysis indicate that: (1) the linear quasi-steady friction effect is more significant than both the nonlinear steady friction and unsteady friction effects for the transient cases with relatively large initial flows (e.g., highly turbulent flows) and relatively small transient intensity (e.g., small perturbations). Under this situation, the linearization assumption becomes valid and accurate for transient modelling and analysis. Otherwise, the nonlinear friction term should be included in the SFR-based modelling and analysis; (2) the unsteady friction effect becomes less important for relatively large scale pipeline systems (e.g., large T_w/T_d or L/D), while nonlinear quasi-steady friction effect is more important for systems with relatively long and small-diameter pipes and highly intensive transients.

5 Further Analysis of the Importance and Influence of Nonlinear Turbulent Friction

Despite that the qualitative insights obtained from the derived extended SFR results in this study, in terms of the importance of nonlinear turbulent friction to transient modelling and analysis, have been widely observed and well expected from previous studies (Ghidaoui et al., 2005; Lee, Duan, Ghidaoui, et al., 2013; Wylie et al., 1993), it is useful and necessary to examine the quantitative trend of its dependence on different parameters under various system and flow conditions, in order to provide a usable and reliable frequency-domain modelling method for full turbulent friction effect. Prior to such systematical analysis, it is a good start to validate the accuracy and validity of the extended SFR-based method through the comparison with the traditional MOC-based simulations.

5.1 Comparison with MOC-based numerical results

The numerical test is conducted based on the MOC-based simulation for the transients caused by full open-and-closure operations at the downstream end shown in Fig. 1 with a wide frequency bandwidth for various flow conditions (Re_0) (e.g., $q_0^* = q_0/Q_0 = 1$). For the illustration and validation purposes, the simple pipe system of reservoir-pipeline-valve as shown in Fig. 1 is used for the analysis, with the pipe parameters given in the figure. The pipeline is assumed to be smooth and the initial friction factor (*f*) is determined by the Colebrook–White equation. The numerical results of transient frequency responses are obtained by the frequency sweeping method based on the MOC-based 1D model in Eq. (1) and Eq. (2) (Lee, Duan, Ghidaoui, et al., 2013). In fact, many previous studies (Chaudhry, 1987; Duan et al., 2014; Duan et al., 2013; Gong et al., 2016; Lee, 2013; Lee et al., 2006; Wylie et al., 1993) have evidenced the difference between the observed results (e.g., by experimental measurement or MOC-based numerical simulation) and the SFR-based transmission modelling results, which is further verified and analyzed in this section. To maintain the accuracy of MOC-based results in the frequency domain, a relative complete transient event with long duration (e.g., 300 wave periods in this study) is required and applied based on the previous findings and discussion in (Lee, Duan, Vítkovský, et al., 2013). Moreover, only the relatively low frequency domain results (e.g., first 10 amplitude peaks) are used for the analysis, which are usually necessary and important to the utilization and analysis of system frequency responses (e.g., leak detection) (Lee, Duan, Ghidaoui, et al., 2013). For this purpose, two test cases of $\mathsf{Re}_0 = 10^4$ and 10^5 are conducted for the validation and analysis, and the results are plotted in Figs 2(a) and 2(b) respectively. More tests are conducted and discussed later in this paper for a wide range of system and flow conditions.

It is necessary to note that, due to the requirements of tremendous computation time and storage space for the convolution process of the WFB unsteady friction model (Ghidaoui et al., 2005; Vardy & Brown, 1995), and the purpose of inspecting nonlinear steady friction effect herein, only the steady friction (linear and nonlinear) effect is considered and tested for the validation through comparisons of analytical and numerical results. The influence of unsteady friction effect will be analyzed later by the validated analytical TFR result in this study. Furthermore, for comparative analysis, two results of linear steady friction only and total (linear and nonlinear) steady friction from the analytical solution are plotted in each figure, so as to highlight the importance and influence of the nonlinear friction effect. Overall, the results of Fig. 2 demonstrate that the inclusion of nonlinear friction term has improved to certain extent the accuracy of SFR-based transient modelling. Specifically, it can be concluded that, compared to the original linear SFR results, much better agreements between the extended SFR results and MOC-based numerical results are obtained for both test cases. By inspection, the average difference of the first 10 peaks is within 6% in comparison with the benchmark values (i.e., numerical results). Nevertheless, small differences still exist, mainly due to the two-step approximation method adopted for the analytical analysis in the appendix (e.g., Eq. (A.19)) which causes the overestimation of nonlinear turbulent friction effect. Moreover, this small difference is almost insensitive to the initial flow conditions (e.g., from $\mathrm{Re}_0 = 10^4$ in Fig. 2a to $\mathrm{Re}_0 = 10^5$ in Fig. 2b);

The preliminary results of Fig. 2 herein have validated the proposed nonlinear turbulent friction derivation for the SFR model. The following sections will investigate and quantify systematically the significance of this improvement compared to the original linearized SFR approach.

5.2 Importance of the improved SFR method

In this section, the linear and nonlinear steady friction components are compared with unsteady friction component to evaluate the importance of the proposed improvement to SFR-based transient modelling. Specifically, the following two expressions are defined and used to evaluate and quantify the relative contribution of the nonlinear turbulent friction model in the frequency domain,

$$\gamma_1(\%) = \frac{P_{s1} - P_{s1s2}}{P_{s1}} \times 100 \tag{19}$$

$$\gamma_2(\%) = \frac{P_{s1} - P_{s1s2}}{P_{s1} - P_{su}} \times 100 \tag{20}$$

where γ_1 is the contribution percentage of the nonlinear turbulence friction damping for the frequency response peaks; γ_2 is the relative importance of the nonlinear turbulent friction to unsteady friction effect; P_{s1}, P_{s1s2}, P_{su} are the frequency domain peak amplitudes of the analytical results with linear steady friction only, total steady friction (linear and nonlinear), and total friction (steady and unsteady), respectively. Both Eq. (19) and Eq. (20) describe, in different expression ways, the contribution of the proposed nonlinear steady friction model to SFR-based transient modelling in the frequency domain. Particularly, γ_1 in Eq. (19) indicates the relative importance of nonlinear steady friction to total steady friction effect (linear and nonlinear steady components), while γ_2 in Eq. (20) represents the relative importance of nonlinear steady friction to total friction effect (steady and unsteady components). For clarity, the test pipe system in Fig. 1 with the case of $\mathsf{Re}_0 = 10^5$ is applied again here for demonstrating various parameters defined in above expressions, which are shown in Fig. 3 by taking the first frequency peak herein for illustration.

According to Eq. (19) and Eq. (20), the individual contribution and relative importance of nonlinear turbulent friction are in principle changing with frequency peak numbers, which is also indicated by the scaling analysis result in Eq. (18). For convenience of the numerical evaluation, the first 6 peaks in the frequency domain for each test case are extracted and used in the following analysis, which represents common situations for transient modeling and analysis (Duan et al., 2011; Lee, Duan, Ghidaoui, et al., 2013). Based on the two evaluation methods, the importance of the proposed nonlinear SFR model can be quantified for various transient conditions (i.e., $q_0^* = q_0/Q_0$). Taking the case of $\mathsf{Re}_0 = 10^5$ in Fig. 1 for illustration, the contribution percentage and relative importance of nonlinear turbulent friction effect under various transient intensity conditions ($q_0^* = q_0/Q_0$) are calculated and plotted in Figs 4(a) and 4(b) respectively.

The results in Fig. 4(a) demonstrate clearly the extended SFR model with nonlinear turbulent friction term increases in importance with the magnitude of the transient event (q_0^*). However, for each imposed transient flow perturbation (q_0^*), the impact of the nonlinear turbulent friction model is constant across all the frequency peaks (i.e., Fig. 4a). This result again confirms the former scaling analysis result of Eq. (18) in this study. In the presence of unsteady friction effect in Fig. 4(b), however, the contribution from the proposed nonlinear steady friction model is decreasing with frequency peak number, which indicates that the importance of nonlinear friction effect is affected by the frequencies of incident waves and system scale configurations.

Furthermore, to investigate the influence of the initial flow conditions (Re_0) and transient generation conditions (q_0^*) in the given pipe system of Fig. 1, the contributions of nonlinear steady friction from the first 6 frequency peaks of each test (e.g., Fig. 4) under various flow conditions are averaged for further analysis. The results are extracted from a

variety of test cases for the system of Fig. 1 and the results from the two evaluation methods are plotted in Figs 5(a) and 5(b) respectively. On the one hand, the overall results of Figs 5(a) and 5(b) confirm further that the impact of the proposed nonlinear turbulent friction model is increasing with transient intensity (q_0^*) for all the test flow conditions. Specifically, the results in Fig. 5 indicate that the average impact of the model (γ_1 and γ_2) attains to over 10% when $q_0^* > 0.3$ for the whole test range of initial flow conditions, which means that the nonlinear turbulent friction effect is important for the frequency domain models. In other words, for this testing pipe system in Fig. 1, the linearization assumption is valid (for say, $\gamma < 1\%$) only when $q_0^* < 0.02$ (i.e., $q_0 < 2\%Q_0$) for the whole test range of initial flow conditions (Re_0), posing a clear limit to the application of the results from previous studies (Duan & Lee, 2016; Duan, Lee, et al., 2012a; Lee et al., 2006; Mpesha et al., 2001; Wang et al., 2002).

Consequently, the results and analysis indicate that the linearization assumption in the SFR-based transient modelling is highly dependent on the initial and transient flow conditions (specifically, Re_0 and Re_{t0}). In the following study, more influence factors are examined and analyzed systematically for the effect of the nonlinear turbulence friction on the SFR results.

5.3 Systematical analysis on factors affecting the importance of nonlinear turbulent friction

The results and analysis in Figs 4 and 5 demonstrate the importance of the derived SFR model with nonlinear turbulent friction under various flow conditions. However, these results and findings are obtained for the specific pipe system in Fig. 1. To generalize the analysis, it is necessary to include more system factors such as pipe scales and fluid properties (e.g., L, D, a, f, v_k).

Based on the scaling analysis in Eq. (16) through Eq. (18), it can be summarized that the individual contribution (R_{s2}) of nonlinear turbulent friction component and its relative importance (η) are dependent on the dimensionless parameters as follows: T_w/T_d (or L/D), $f\mathrm{Re}_0$ (or $f\mathrm{M}$), and Re_{t0} (or q_0^*). The dependence of the nonlinear turbulent friction model on these factors is calculated for typical ranges of these parameters in practical water pipeline systems. The obtained results are shown in Figs 6 and 7 respectively, where the relative importance indicators (γ_1 and γ_2) defined previously in Eq. (19) and Eq. (20) are adopted for the analysis.

The results of Figs 6 and 7 confirm further the previous findings on the dependence of the influence of nonlinear turbulent friction component on the initial and transient flow conditions ($f\mathrm{Re}_0$ and q_0^*). In particular, the results of Figs (6a) and (7a) indicate that the contribution percentage (γ_1) of nonlinear turbulent friction is almost constant with both the factors of system scales (T_w/T_d or L/D) and initial flow conditions ($f\mathrm{Re}_0$), but is increasing

with transient conditions (q_0^* or Re_{t0}). However, the results of Figs (6b) and (7b) reveal clearly that the relative importance (γ_2) to the unsteady friction effect is increasing with system scales (T_w/T_d or L/D), especially for the highly turbulent and transient flow conditions. Overall, the comparison of the results in Figs 6 and 7 demonstrate that the influence of nonlinear friction effect (both γ_1 and γ_2) is more sensitive to the transient intensity condition (q_0^* or Re_{t0}) than the system scales (T_w/T_d or L/D) and initial flow conditions ($f\mathrm{Re}_0$). In other words, the size (or intensity extent) of the transient event is the driving factor behind the importance of nonlinear turbulent friction component in the SFR-based transient modelling and analysis, followed subsequently by the factors of the initial flow condition ($f\mathrm{Re}_0$) and the system scales (T_w/T_d or L/D). Therefore, for practical water supply pipeline systems where these three factors (T_w/T_d or L/D, q_0^* or Re_{t0}, $f\mathrm{Re}_0$or $f\mathrm{M}$) are very case-sensitive and time-dependent, it is necessary to consider and include the influence of nonlinear turbulent friction term, in addition to the linear steady and unsteady friction components in original SFR, for achieving better accuracy of transient modelling and analysis. From this perspective, the results of Figs 6 and 7 and the extended SFR in Eq. (15) in this study may provide useful basis and substantial evidence for such consideration.

6 Results Discussion and Implications

The results and analysis above have demonstrated the accuracy improvement of the extended SFR model for the transient analysis, and meanwhile, indicated the importance of nonlinear turbulent frictions to frequency domain transient responses under various system and flow conditions. Specifically, following implications may be obtained from this study:

(1) Development of transient friction model, especially for the frequency domain transient modelling and analysis. On the one hand, the results and analysis of this study confirm the previous understanding and results in the literature with regard to the frequency-independence of steady friction effect on transient responses. On the other hand, the analytical results obtained in this study may provide additional insights for various experimental observations of more fast and severe transient attenuation in the frequency domain than the traditional linear SFR results in the literature (Duan et al., 2013; Lee et al., 2006);

(2) Application of SFR-based transient modelling and analysis in theoretical and practical pipe systems. This study provides a systematic and scientific way to judge the cases in which the nonlinear friction term is important or not to the transient modelling and analysis (e.g., Figs 6 and 7). For the cases where the nonlinear steady friction is important, the extended SFR developed in this study can then provide an accurate and

efficient way to include this influence factor in the modelling and analysis of these transient systems, i.e., Eq. (15) or Eq. (A.30);

(3) Further understanding of unsteady turbulence in transients. From the scaling analysis results in Eq. (16) and Eq. (17), it is shown that the nonlinear steady friction (turbulence) term is time dependent for its influence and importance, particularly, relating to transient intensity (Re_{t0}) and system scales (T_w/T_d). Note that the unsteady friction was also found to be related to these two factors in previous studies (Duan, Ghidaoui, et al., 2012; Meniconi et al., 2014; Vardy & Brown, 1995). As a result, a scientific connection of various physical mechanisms such as unsteady turbulence generation and kinematic diffusion may be established between these two friction components for interpreting transient evolution and process.

7 Summary and Conclusions

This paper investigates the influence and importance of the nonlinear steady friction component in the SFR-based transient modelling and analysis. In this study, analytical derivation is firstly conducted for improving and extending the SFR result by including the nonlinear turbulent friction term based on a two-step approximation method. The extended SFR result is then validated fully by the MOC-based numerical simulations in the frequency domain.

The obtained results of this study have provided further evidence and confirmation to the influence of nonlinear turbulent friction on SFR widely observed in previous numerical and experimental studies, and developed a usable and reliable modelling method for nonlinear turbulent friction effect in the frequency domain. Specifically, the results analysis and discussion demonstrate the improvement of the accuracy and validity of the extended SFR result for representing the nonlinear steady friction effect. Moreover, the scaling analysis for the extended SFR result indicates that the potential influence and importance of nonlinear steady friction term is highly dependent on the factors of transient intensity and system scales.

Furthermore, based on the extended SFR in this study, a systematical analysis is performed for analyzing the factors affecting and governing the contribution and importance of nonlinear turbulent friction term in the frequency-domain transmission line modelling and analysis. As indicated from the scaling analysis, three common factors of system scales, initial flow and transient conditions are examined in the analysis for their typical influence ranges in practical water pipeline systems. The application results indicate that the relative influence of the nonlinear turbulent friction is increasing with both initial and transient flow conditions ($f\mathrm{Re}_0$, q_0^*), but remains relatively constant with system scales (T_w/T_d or L/D) and incident wave frequency (ω).

The results and analysis of this study may provide scientific basis and useful alternative to the development and utilization of the SRF-based method for transient pipe flow modelling and analysis, as well as pipe condition assessment such as pipe leakage and blockage detection in the field of urban water pipeline systems.

Acknowledgements

This research was supported by the research grants from: (1) the Hong Kong Polytechnic University (HKPU) under the projects no. 1-ZVCD, no. 1-ZVGF and no. 3-RBAB; and (2) the Hong Kong Research Grant Council (RGC) under the projects no. T21-602/15-R, no. 25200616 and no. 15201017.

Appendix – Analytical Derivation of Extended SFR Result

Combination of Eqs (1) through (5) gives,

$$\frac{gA}{a^2}\frac{\partial H}{\partial t}+\frac{\partial Q}{\partial x}=0 \tag{A.1}$$

$$\frac{1}{gA}\frac{\partial Q}{\partial t}+\frac{\partial H}{\partial x}+sign(Q)\frac{fQ^2}{2gDA^2}+C_J\int_0^t W\left(t-t'\right)\frac{\partial Q}{\partial t'}dt'=0 \tag{A.2}$$

where $C_J = 16\nu/gD^2A$. In transient pipe flows, the variables H and Q can be expressed as:

$$H = H_0 + h \tag{A.3}$$

$$Q = Q_0 + q \tag{A.4}$$

where H_0 is mean pressure head; h is transient pressure head; Q_0 is mean pipe discharge (defined as positive for initial flow state); q is instantaneous transient discharge, which is same as the defined q_t in Eq. (9) with subscript t neglected here for simplicity.

Note that the mean quantities of discharge and pressure head are time independent, such that the terms related to $\partial Q_0/\partial x$, $\partial Q_0/\partial t$ and $\partial Q_0/\partial t$ in above equations are all zero. Therefore,

$$\frac{\partial Q}{\partial t}=\frac{\partial q}{\partial t},\ \frac{\partial Q}{\partial x}=\frac{\partial q}{\partial x} \tag{A.5}$$

$$\frac{\partial H}{\partial t}=\frac{\partial h}{\partial t},\ \frac{\partial H}{\partial x}=\frac{\partial H_0}{\partial x}+\frac{\partial h}{\partial x} \tag{A.6}$$

$$\frac{\partial H_0}{\partial x}=-sign(Q_0)\frac{fQ_0^2}{2gDA^2} \tag{A.7}$$

Substituting Eq. (A.3) through Eq. (A.7) into Eqs (A.1) and (A.2) gives,

$$\frac{gA}{a^2}\frac{\partial h}{\partial t}+\frac{\partial q}{\partial x}=0 \tag{A.8}$$

$$\frac{1}{gA}\frac{\partial q}{\partial t}+\frac{\partial h}{\partial x}+sign(Q)\frac{f}{2gDA^2}\left(2Q_0q+q^2\right)+C_J\int_0^t W\left(t-t'\right)\frac{\partial q}{\partial t'}dt'=0 \tag{A.9}$$

Applying Fourier transform to Eqs (A.8) and (A.9) provides,

$$i\omega\frac{gA}{a^2}h^*+\frac{\partial q^*}{\partial x}=0 \tag{A.10}$$

$$i\omega\frac{1}{gA}q^*+\frac{\partial h^*}{\partial x}+\frac{fQ_0}{gDA^2}q^*+sign(Q)\frac{f}{2gDA^2}\left(q^2\right)^*+i\omega\frac{\phi C_J}{\sqrt{\pi}\sqrt{\lambda+i\omega}}q^*=0 \tag{A.11}$$

where $i=\sqrt{-1}$ is imaginary unit; ω is frequency; h^* and q^* are transformed quantities of h and q in the frequency domain respectively. To solve these equations, the nonlinear term $(q^2)^*$ is determined by the following two-step approximation:

(1) Step 1: By ignoring $(q^2)^*$, Eqs (A.10) and (A.11) become linear forms as follows:

$$i\omega\frac{gA}{a^2}h^*+\frac{\partial q^*}{\partial x}=0 \tag{A.12}$$

$$i\omega\frac{1}{gA}q^*+\frac{\partial h^*}{\partial x}+sign(Q)\frac{fQ_0}{gDA^2}q^*+i\omega\frac{\phi C_J}{\sqrt{\pi}\sqrt{\lambda+i\omega}}q^*=0 \tag{A.13}$$

Eliminating h^* from Eqs (A.12) and (A.13) by,

$$\frac{\partial(\text{A12})}{\partial x}-(\text{A13})\times\left(i\omega\frac{gA}{a^2}\right)=0 \tag{A.14}$$

leads to,

$$\frac{\partial^2 q^*}{\partial x^2}+C_Q q^*=0 \tag{A.15}$$

where $C_Q=\frac{\omega^2}{a^2}\left[1-i\left(sign(Q)\frac{fQ_0}{\omega DA}+\frac{igA\phi C_J}{\sqrt{\pi}\sqrt{\lambda+i\omega}}\right)\right]$.

The solution for Eq. (A.15) has the following form (Duan, Ghidaoui, et al., 2012),

$$q^*(x,\omega)=q_0^*e^{-Kx\omega} \tag{A.16}$$

where $K=\sqrt{-C_Q/\omega^2}$ is the propagation factor of transient waves.

(2) Step 2: using the linear solution of Eq. (A.16) to estimate the term $(q^2)^*$ in Eq. (A.11) above. Particularly for transients caused by sudden valve closure (partial or full closure)

$$q(x=0)=q_0(t)=q_{t0} \tag{A.17}$$

where q_{t0} is transient flowrate change at $x = 0$ as defined in Eq. (14). Under this condition, it has $sign(Q) = 1$ (i.e., $|q_{t0}| \le Q_0$). Therefore,

$$q_0^*(\omega)=\hat{q}_0=\int_{-\infty}^{+\infty}q_0e^{-i\omega t}dt=\int_{-\infty}^{+\infty}q_{t0}e^{-i\omega t}dt=|q_{t0}|\delta(\omega) \tag{A.18}$$

where $\delta(\omega)$ is delta function. As a result,

$$\left(q^2\right)^*=q^*\otimes q^*=\int_0^{\omega}\left[|q_{t0}|\delta(\tau)e^{-Kx\tau}\right]\left[|q_{t0}|\delta(\omega-\tau)e^{-Kx(\omega-\tau)}\right]d\tau=|q_{t0}|q^* \tag{A.19}$$

With this result, Eqs (A.10) and (A.11) can be rewritten as

$$i\omega\frac{gA}{a^2}h^*+\frac{\partial q^*}{\partial x}=0 \tag{A.20}$$

$$i\omega\frac{1}{gA}q^*+\frac{\partial h^*}{\partial x}+\left(\frac{fQ_0}{gDA^2}+\frac{fq_{t0}}{2gDA^2}\right)q^*+i\omega\frac{\phi C_J}{\sqrt{\pi(\lambda+i\omega)}}q^*=0 \tag{A.21}$$

Applying the similar elimination process in Eq. (A.14), gives,

$$\frac{\partial^2 q^*}{\partial x^2}+\mu_E^2q^*=0 \tag{A.22}$$

where $\mu_E^2=\frac{\omega^2}{a^2}\left[1-i\left(\frac{fQ_0}{\omega DA}+\frac{fq_{t0}}{2\omega DA}+\frac{igA\phi C_J}{\sqrt{\pi}\sqrt{\lambda+i\omega}}\right)\right]$.

Consequently, the solution of Eq. (A.22) can be expressed as

$$q^*=C_1\sinh(i\mu_Ex)+C_2\cosh(i\mu_Ex) \tag{A.23}$$

where C_1, C_2 are arbitrary constants, which relate to the system boundary conditions. Substituting Eq. (A.23) into Eq. (A.10) or Eq. (A.20) gives,

$$h^*=-\frac{a^2\mu_E}{i\omega gA}\left[C_1\cosh(i\mu_Ex)+C_2\sinh(i\mu_Ex)\right] \tag{A.24}$$

It is assumed that, at the upstream end (with superscript "*U*") of the i^{th} pipe section (i.e., $x = 0$), the boundary conditions are

$$h^*=h_i^{*U};\ q^*=q_i^{*U} \tag{A.25}$$

which results in the coefficients C_1 and C_2, as,

$$C_1 = -\frac{\omega g A_i}{a_i^2 \mu_{Ei}} h_i^{*U},\ C_2 = q_i^{*U} \tag{A.26}$$

Similarly, at the downstream end (with superscript "D") of the i^{th} pipe section (i.e., $x = l_i$), it has,

$$h^* = h_{i+1}^{*D};\ q^* = q_{i+1}^{*D} \tag{A.27}$$

Therefore, Eqs (A.23) and (A.24) become

$$q_{i+1}^{*D} = \cosh(i\mu_{Ei} l_i) q_i^{*U} + \frac{1}{Z_E} \sinh(i\mu_{Ei} l_i) h_i^{*U} \tag{A.28}$$

$$h_{i+1}^{*D} = Z_E \sinh(i\mu_{Ei} l_i) q_i^{*U} + \cosh(i\mu_{Ei} l_i) h_i^{*U} \tag{A.29}$$

where $Z_E = -\frac{\mu_{Ei} a_i^2}{\omega g A_i}$.

In matrix form, the results of Eqs (A.28) and (A.29) can be written as,

$$\begin{Bmatrix} q^* \\ h^* \end{Bmatrix}_i^D = \begin{bmatrix} \cosh(i\mu_{Ei} l_i) & \frac{1}{Z_E} \sinh(i\mu_{Ei} l_i) \\ Z_E \sinh(i\mu_{Ei} l_i) & \cosh(i\mu_{Ei} l_i) \end{bmatrix} \begin{Bmatrix} q^* \\ h^* \end{Bmatrix}_i^U \tag{A.30}$$

Notation

a = wavespeed (ms^{-1})

A = pipe cross-sectional area (m^2)

D = pipe diameter (m)

f = Darcy friction factor at initial flow state (-)

g = gravitational acceleration (ms^{-2})

h = transient pressure head (m)

h^* = transient head in the frequency domain (m)

H = pressure head (m)

H_0 = mean pressure head (m)

i = imaginary unit (-)

l = length of uniform pipe section (m)

M = Mach number (-)

q = instantaneous transient discharge (m^3s^{-1})

q_t = transient flow part (m^3s^{-1})

q_t^* = the percentage of transient part in the total flow (-)

Q = flowrate (m^3s^{-1})

Q_0 = mean pipe discharge (m^3s^{-1})

Re_0 = Reynolds number for initially steady state (-)

Re_{t0}= critical Reynolds number for the generated transient flow state (-)

t = time (s)

T_d = radial kinematic diffusion time scale (s)

T_w = longitudinal wave time scale (s)

x = spatial coordinate along pipeline (m)

v = kinematic viscosity ($kgm^{-1}s^{-1}$)

ρ = fluid density (kgm^{-3})

τ_w = pipe wall shear stress (Pa)

ω = frequency ($rads^{-1}$)

References

Brunone, B. (1999). Transient test-based technique for leak detection in outfall pipes. Journal of Water Resources Planning and Management, 125(5), 302-306. doi:10.1061/(ASCE)0733-9496(1999)125:5(302)

Chaudhry, M. H. (1987). Applied Hydraulic Transients. New York: Van Nostrand Reinhold.

Colombo, A. F., Lee, P. J., & Karney, B. W. (2009). A selective literature review of transient-based leak detection methods. Journal of Hydro-environment Research, 2(4), 212-227. doi:10.1016/j.jher.2009.02.003

Covas, D., Ramos, H., Graham, N., & Maksimovic, C. (2005). Application of hydraulic transients for leak detection in water supply systems. Water Science and Technology: Water Supply, 4(5-6), 365-374. Retrieved from http://ws.iwaponline.com/

Duan, H. F., Ghidaoui, M. S., Lee, P. J., & Tung, Y. K. (2010). Unsteady friction and visco-elasticity in pipe fluid transients. Journal of Hydraulic Research, 48(3), 354-362. doi:10.1080/00221681003726247

Duan, H. F., Ghidaoui, M. S., Lee, P. J., & Tung, Y. K. (2012). Relevance of unsteady friction to pipe size and length in pipe fluid transients. Journal of Hydraulic Engineering, 138(2), 154-166. doi:10.1061/(ASCE)HY.1943-7900.0000497

Duan, H. F., & Lee, P. J. (2016). Transient-Based Frequency Domain Method for Dead-End Side Branch Detection in Reservoir Pipeline-Valve Systems. Journal of Hydraulic Engineering, 142(2), 04015042. doi:10.1061/(ASCE)HY.1943-7900.0001070

Duan, H. F., Lee, P. J., Ghidaoui, M. S., & Tuck, J. (2014). Transient wave-blockage interaction and extended blockage detection in elastic water pipelines. Journal of fluids and structures, 46(2014), 2-16. doi:10.1016/j.jfluidstructs.2013.12.002

Duan, H. F., Lee, P. J., Ghidaoui, M. S., & Tung, Y. K. (2010). Essential system response information for transient-based leak detection methods. Journal of Hydraulic Research, 48(5), 650-657. doi:10.1080/00221686.2010.507014

Duan, H. F., Lee, P. J., Ghidaoui, M. S., & Tung, Y. K. (2011). Leak detection in complex series pipelines by using the system frequency response method. Journal of Hydraulic Research, 49(2), 213-221. doi:10.1080/00221686.2011.553486

Duan, H. F., Lee, P. J., Ghidaoui, M. S., & Tung, Y. K. (2012a). Extended blockage detection in pipelines by using the system frequency response analysis. Journal of Water Resources Planning and Management, 138(1), 55-62. doi:10.1061/(ASCE)WR.1943-5452.0000145

Duan, H. F., Lee, P. J., Ghidaoui, M. S., & Tung, Y. K. (2012b). System response function–based leak detection in viscoelastic pipelines. Journal of Hydraulic Engineering, 138(2), 143-153. doi:10.1061/(ASCE)HY.1943-7900.0000495

Duan, H. F., Lee, P. J., Kashima, A., Lu, J. L., Ghidaoui, M. S., & Tung, Y. K. (2013). Extended blockage detection in pipes using the system frequency response: analytical analysis and experimental verification. Journal of Hydraulic Engineering, 139(7), 763-771. doi:10.1061/(ASCE)HY.1943-7900.0000736

Duan, H. F., Tung, Y. K., & Ghidaoui, M. S. (2010). Probabilistic analysis of transient design for water supply systems. Journal of Water Resources Planning and Management, 136(6), 678-687. doi:10.1061/(ASCE)WR.1943-5452.0000074

Ferrante, M., & Brunone, B. (2003). Pipe system diagnosis and leak detection by unsteady-state tests. 1. Harmonic analysis. Advances in Water Resources, 26(1), 95-105. doi:10.1016/S0309-1708(02)00101-X

Ghazali, M. F., Beck, S. B. M., Shucksmith, J. D., Boxall, J. B., & Staszewski, W. J. (2012). Comparative study of instantaneous frequency based methods for leak detection in pipeline networks. Mechanical Systems and Signal Processing, 29, 187-200. doi:10.1016/j.ymssp.2011.10.011

Ghidaoui, M. S., & Mansour, S. (2002). Efficient treatment of the Vardy–Brown unsteady shear in pipe transients. Journal of Hydraulic Engineering, 128(1), 102-112. doi:10.1061/(ASCE)0733-9429(2002)128:1(102

Ghidaoui, M. S., Zhao, M., McInnis, D. A., & Axworthy, D. H. (2005). A review of water hammer theory and practice. Applied Mechanics Reviews, 58, 49-76. doi:10.1115/1.1828050

Gong, J., Lambert, M. F., Zecchin, A. C., & Simpson, A. R. (2016). Experimental verification of pipeline frequency response extraction and leak detection using the inverse repeat signal. Journal of Hydraulic Research, 54(2), 210-219. doi:10.1061/(ASCE)HY.1943-7900.0000736

Kim, S. (2007). Impedance matrix method for transient analysis of complicated pipe networks. Journal of Hydraulic Research, 45(6), 818-828. doi:10.1080/00221686.2007.9521819

Lee, P. J. (2013). Energy analysis for the illustration of inaccuracies in the linear modelling of pipe fluid transients. Journal of Hydraulic Research, 51(2), 133-144. doi:10.1080/00221686.2012.734861

Lee, P. J., Duan, H. F., Ghidaoui, M. S., & Karney, B. W. (2013). Frequency domain analysis of pipe fluid transient behaviour. Journal of Hydraulic Research, 51(6), 609-622. doi:10.1080/00221686.2013.814597

Lee, P. J., Duan, H. F., Vítkovský, J. P., Zecchin, A. C., & Ghidaoui, M. S. (2013). The effect of time–frequency discretization on the accuracy of the transmission line modelling of fluid transients. Journal of Hydraulic Research, 51(3), 273-283. doi:10.1080/00221686.2012.749430

Lee, P. J., Lambert, M. F., Simpson, A. R., Vítkovský, J. P., & Liggett, J. A. (2006). Experimental verification of the frequency response method for pipeline leak detection. Journal of Hydraulic Research, 44(5), 693-707. doi:10.1080/00221686.2006.9521718

Lee, P. J., & Vítkovský, J. P. (2010). Quantifying linearization error when modeling fluid pipeline transients using the frequency response method. Journal of Hydraulic Engineering, 136(10), 831-836. doi:10.1061/(ASCE)HY.1943-7900.0000246

Lee, P. J., Vítkovský, J. P., Lambert, M. F., Simpson, A. R., & Liggett, J. A. (2005). Frequency domain analysis for detecting pipeline leaks. Journal of Hydraulic Engineering, 131(7), 596-604. doi:10.1061/(ASCE)0733-9429(2005)131:7(596)

Meniconi, S., Brunone, B., Ferrante, M., Capponi, C., Carrettini, C. A., Chiesa, C., . . . Lanfranchi, E. A. (2015). Anomaly pre-localization in distribution–transmission mains by pump trip: preliminary field tests in the Milan pipe system. Journal of Hydroinformatics, 17(3), 377-389. doi:10.2166/hydro.2014.038

Meniconi, S., Brunone, B., Ferrante, M., & Massari, C. (2011). Potential of transient tests to diagnose real supply pipe systems: What can be done with a single extemporary test. Journal of Water Resources Planning and Management, 137(2), 238-241. doi:10.1061/(ASCE)WR.1943-5452.0000098

Meniconi, S., Duan, H. F., Brunone, B., Ghidaoui, M. S., Lee, P. J., & Ferrante, M. (2014). Further developments in rapidly decelerating turbulent pipe flow modeling. Journal of Hydraulic Engineering, 140(7), 04014028. doi:10.1061/(ASCE)HY.1943-7900.0000880

Mpesha, W., Gassman, S. L., & Chaudhry, M. H. (2001). Leak detection in pipes by frequency response method. Journal of Hydraulic Engineering, 127(2), 134-147. doi:10.1061/(ASCE)0733-9429(2001)127:2(134)

Sattar, A. M., & Chaudhry, M. H. (2008). Leak detection in pipelines by frequency response method. Journal of Hydraulic Research, 46(EI1), 138-151. doi:10.1080/00221686.2008.9521948

Vardy, A. E., & Brown, J. M. B. (1995). Transient, turbulent, smooth pipe friction. Journal of Hydraulic Research, 33(4), 435-456. doi:10.1080/00221689509498654

Vardy, A. E., & Brown, J. M. B. (2003). Transient turbulent friction in smooth pipe flows. Journal of Sound and Vibration, 259(5), 1011-1036. doi:10.1006/jsvi.2002.5160

Vítkovský, J. P., Lee, P. J., Zecchin, A. C., Simpson, A. R., & Lambert, M. F. (2011). Head- and flow-based formulations for frequency domain analysis of fluid transients in arbitrary pipe networks. Journal of Hydraulic Engineering, 137(5), 556-568. doi:10.1061/(ASCE)HY.1943-7900.0000338

Vítkovský, J. P., Simpson, A. R., & Lambert, M. F. (2000). Leak detection and calibration using transients and genetic algorithms. Journal of Water Resources Planning and Management, 126(4), 262-265. doi:10.1061/(ASCE)0733-9496(2000)126:4(262)

Vítkovský, J. P., Stephens, M., Bergant, A., Simpson, A. R., & Lambert, M. F. (2006). Numerical error in weighting function-based unsteady friction models for pipe transients. Journal of Hydraulic Engineering, 132(7), 709-721. doi:10.1061/(ASCE)0733-9429(2006)132:7(709)

Wang, X. J., Lambert, M. F., Simpson, A. R., Liggett, J. A., & Vítkovský, J. P. (2002). Leak detection in pipelines using the damping of fluid transients. Journal of Hydraulic Engineering, 128(7), 697-711. doi:10.1061/(ASCE)0733-9429(2002)128:7(697)

Wylie, E. B., Streeter, V. L., & Suo, L. S. (1993). Fluid Transients in Systems. Englewood Cliffs, New Jersey: Prentice-Hall.

Zecchin, A. C., Lambert, M. F., Simpson, A. R., & White, L. B. (2010). Frequency-domain modeling of transients in pipe networks with compound nodes using a Laplace-domain admittance matrix. Journal of Hydraulic Engineering, 136(10), 739-755. doi:10.1061/(ASCE)HY.1943-7900.0000248

Zielke, W. (1968). Frequency-dependent friction in transient pipe flow. Journal of Basic Engineering, 90(1), 109-115. doi:10.1115/1.3605049

List of figures

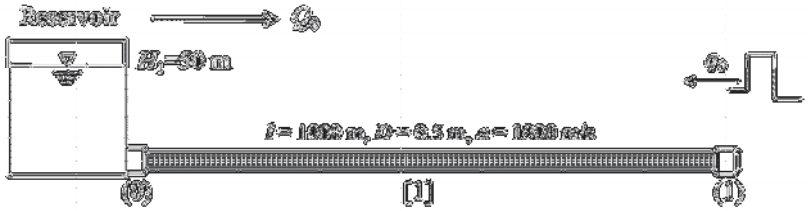

Figure 1 Schematic of reservoir-pipeline-valve system

215x47mm (300 x 300 DPI)

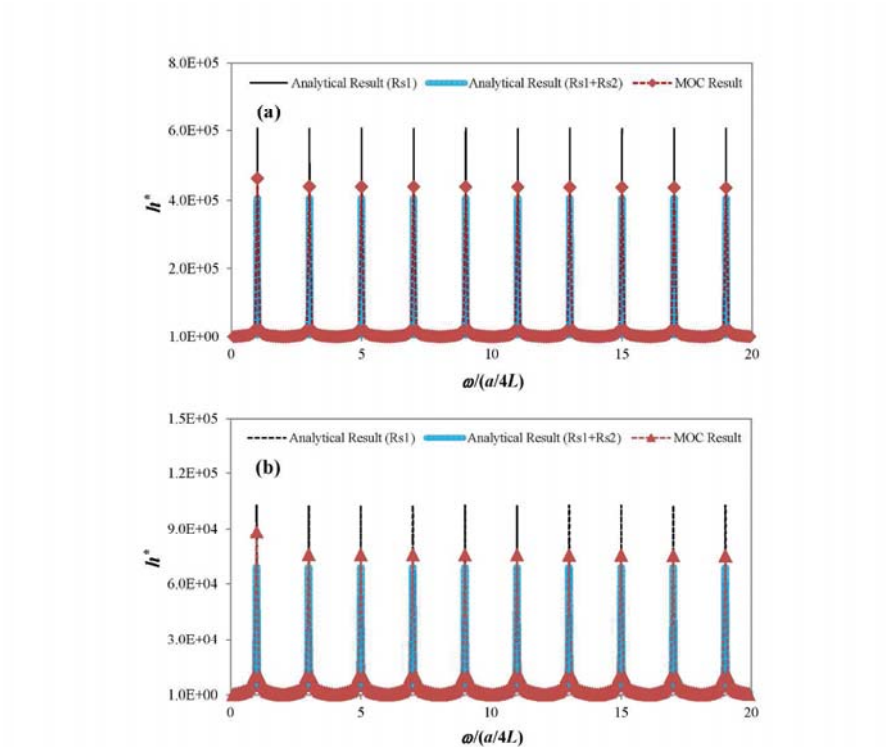

Figure 2 SFR results by the analytical solution and the MOC-based simulation for: (a) $Re_0 = Re_{t0} = 10^4$; (b) $Re_0 = Re_{t0} = 10^5$

215x279mm (300 x 300 DPI)

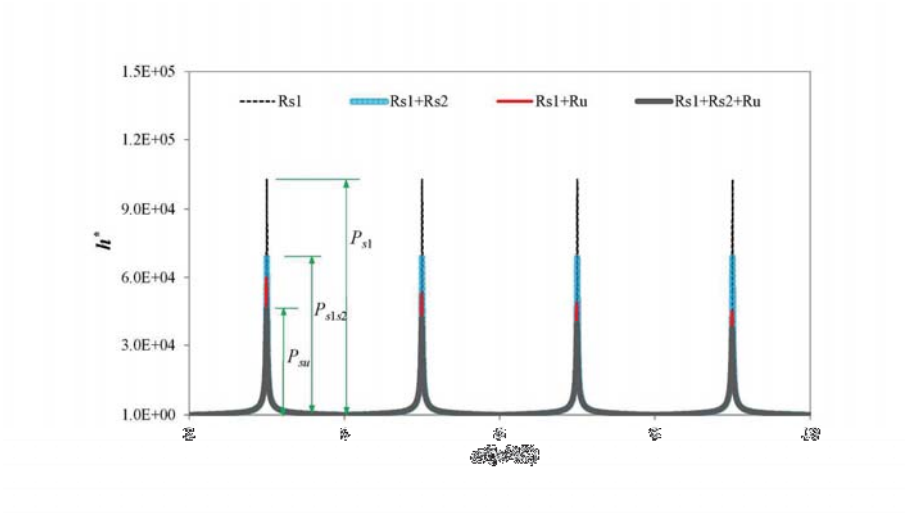

Figure 3 Illustration of SFR results for different friction component effects ($Re_0 = Re_{t0} = 10^5$)

215x279mm (300 x 300 DPI)

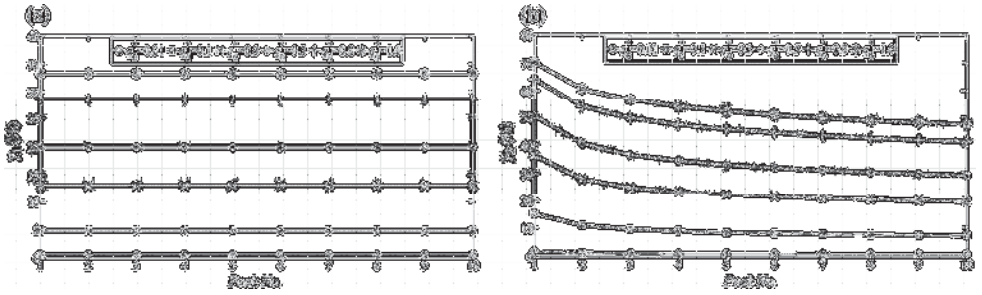

Figure 4 Variation trend of the influence of nonlinear turbulent friction component with frequency for $Re_0 = 10^5$ under various transient conditions: (a) contribution percentage to the frequency peak (γ_1); (b) relative importance to unsteady friction (γ_2)

165x48mm (300 x 300 DPI)

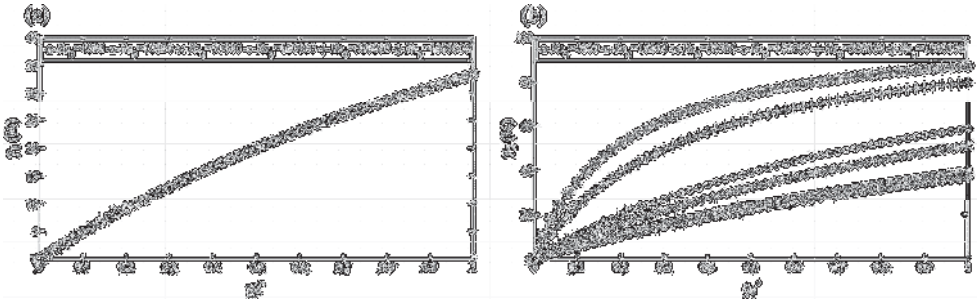

Figure 5 Variation trend of the frequency domain averaged influence of nonlinear turbulent friction component with initial flow and transient conditions: (a) contribution percentage to the frequency peak (γ_2); (b) relative importance to unsteady friction (γ_2)

165x50mm (300 x 300 DPI)

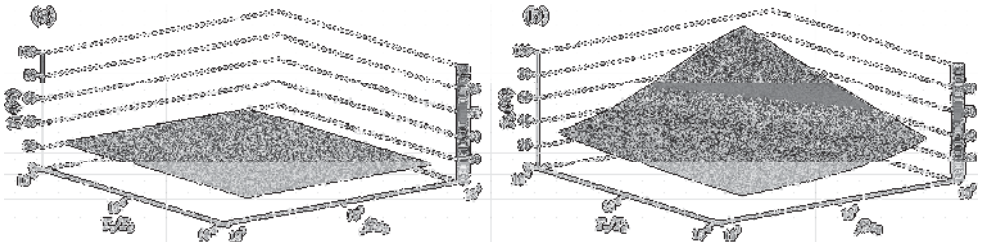

Figure 6 Variation of the contribution of nonlinear turbulent friction component with initial flow conditions and system properties for q_0* =0.5: (a) contribution percentage to the frequency peak (γ_1); (b) relative importance to unsteady friction (γ_2)

172x42mm (300 x 300 DPI)

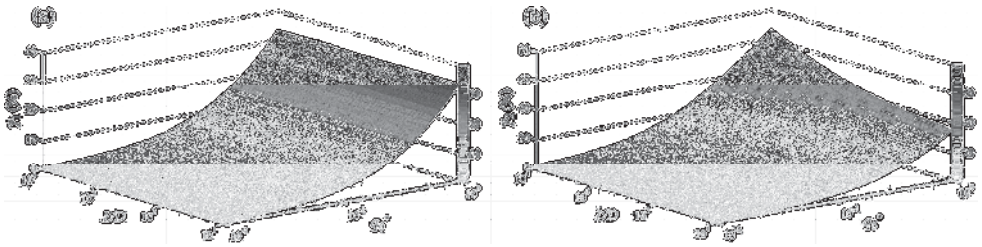

Figure 7 Variation of the contribution of nonlinear turbulent friction component with relative transient intensity and system scale for $Re_0 = 10^5$: (a) contribution percentage to the frequency peak (γ_1); (b) relative importance to unsteady friction (γ_2)

173x42mm (300 x 300 DPI)